purchased from Applied Biosystems. Expression was normalized using *Ubiquitin C*.

Statistical Analysis

All values are expressed as mean±SEM. Statistical comparison of the data was performed using the student's unpaired *t*-test for the analysis of circulating HMGB1 levels. All other data were analyzed with one-way ANOVA followed by Fisher's post-hoc analysis to compare groups. A value of $p<0.05$ was considered statistically significant.

Results

Poor Donor Cell Survival and Increased Extracellular HMGB1 After BMC Transplantation

Female rats suffering ischemic cardiomyopathy were randomly assigned to 4 groups; intramyocardial injection of syngeneic male BMCs (BMC group), intramyocardial injection of male BMCs with anti-HMGB1 neutralizing antibody (AB group), intramyocardial injection of male BMCs with control IgG (IgG group), and intramyocardial injection of PBS only (CON group). After each treatment, quantitative PCR for the male-specific *sry* gene demonstrated that donor cell survival after BMC transplantation was poor similarly in the BMC, AB, and IgG groups; below 10% at day 3, further decreasing to below 1% by day 28 (**Figure 1A**). Histological analysis detected islet-like clusters of donor cells at day 3 after BMC transplantation (**Figure 1B**). ELISA showed that the circulating extracellular HMGB1 level was 2.5-fold elevated one hour after BMC transplantation, compared to the PBS injection control (**Figure 1C**).

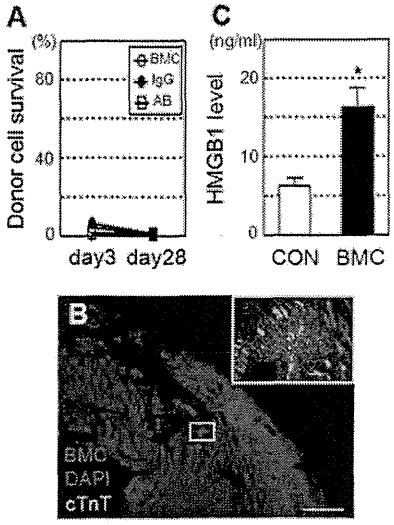

Figure 1. Poor donor cell survival and HMGB1 leakage after BMC transplantation. (**A**) Quantitative PCR for the male specific *sry* gene showed that the survival of male donor cells in female hearts was poor similarly in the BMC (BMC injection), IgG (BMC+control IgG injection), and AB (BMC+anti-HMGB1 antibody injection) groups at both days 3 and 28; n=5~7 in each point. (**B**) Clusters of DiI-labeled (red) donor BMCs were detected in the heart at day 3 after BMC transplantation. A higher magnification image of the yellow frame is shown. Green=cardiomyocytes (cTnT); blue=nuclei (DAPI). Scale bar=300 μm. (**C**) ELISA showed that the circulating HMGB1 level was increased at 1 hour in the BMC group compared to the PBS injection control (CON group). *:$p<0.05$ *versus* the CON group, mean±SEM for n=5 each.
doi:10.1371/journal.pone.0076908.g001

Abolished BMC Transplantation-induced Cardiac Function Recovery by HMGB1-inhibition

Four weeks after BMC transplantation (BMC group), echocardiography and cardiac catheterization consistently demonstrated that both systolic and diastolic LV function, in terms of LV fractional area change, max and min dP/dt, and systolic pressure, was improved compared to the control (CON group; **Figure 2**). Enlargement of LV systolic endocardial area in the control group was attenuated by BMC transplantation. Of note, these effects were largely abolished by HMGB1-inhibition (AB group), but not by control IgG administration (IgG group), indicating an important role of extracellular HMGB1 in the therapeutic benefits of BMC transplantation.

Elimination of BMC Transplantation-induced Tissue Recovery by HMGB1-inhibition

To investigate the mechanism by which extracellular HMGB1 released in BMC transplantation improved post-MI cardiac function, we performed a set of histological studies with a focus on the paracrine effect. Consistent to previous reports [3], BMC transplantation (BMC group) attenuated post-MI pathological fibrosis, improved neovascular formation, and increased proliferation activity in the border areas at day 28, compared to the control (CON group; **Figure 3 and Figure S2**). All these paracrine effects were, however, eliminated by HMGB1-inhibition (AB group), but not by IgG administration (IgG group), corresponding to the cardiac function change as shown in Figure 2.

Modulation of M2/M1 Macrophage Polarization by BMC Transplantation through HMGB1

Additional immunolabeling showed that BMC transplantation increased myocardial accumulation of $CD68^+$ pan-macrophages compared to the control (**Figure 4A and Figure S3A, B**). Here, the increase in $CD86^+$ classically-activated pro-inflammatory (M1) macrophages was trivial (**Figure 4B and Figure S3D, E**), while the enhancement of $CD163^+$ alternatively-activated (M2) macrophages was more obvious (**Figure 4C and Figure S3G, H**). As a result, the ratio of M2/M1 macrophage in the BMC group (92.9/36.9=2.52) was increased from 56.3/28.4=1.98 in the CON group. Of note, HMGB1-inhibition abolished the enhancement of $CD163^+$ M2 macrophages (**Figure 4C and Figure S3I**) and exacerbated the increase in $CD86^+$ M1 macrophages (**Figure 4B and Figure S3F**), thus largely reducing the M2/M1 ratio to 67.6/62.9=1.07. These results suggest that the HMGB1-mediated shift of macrophage polarization towards anti-inflammatory M2 macrophages might play a role in the BMC transplantation-induced myocardial recovery.

Quantitative RT-PCR showed that myocardial expression of the anti-inflammatory cytokine, *IL-10*, tended to be elevated by BMC transplantation compared to the control, while this was totally eliminated by inhibiting HMGB1 (**Figure 4D**). IL-10 is known to be secreted by alternatively activated M2 macrophages and also by Th2 cells that induce M2 macrophage differentiation [9,25,26]. The expression of *IL-1β* or *TNF-α* was not affected by either BMC transplantation or HMGB1-inhibition (**Figure 4E, F**).

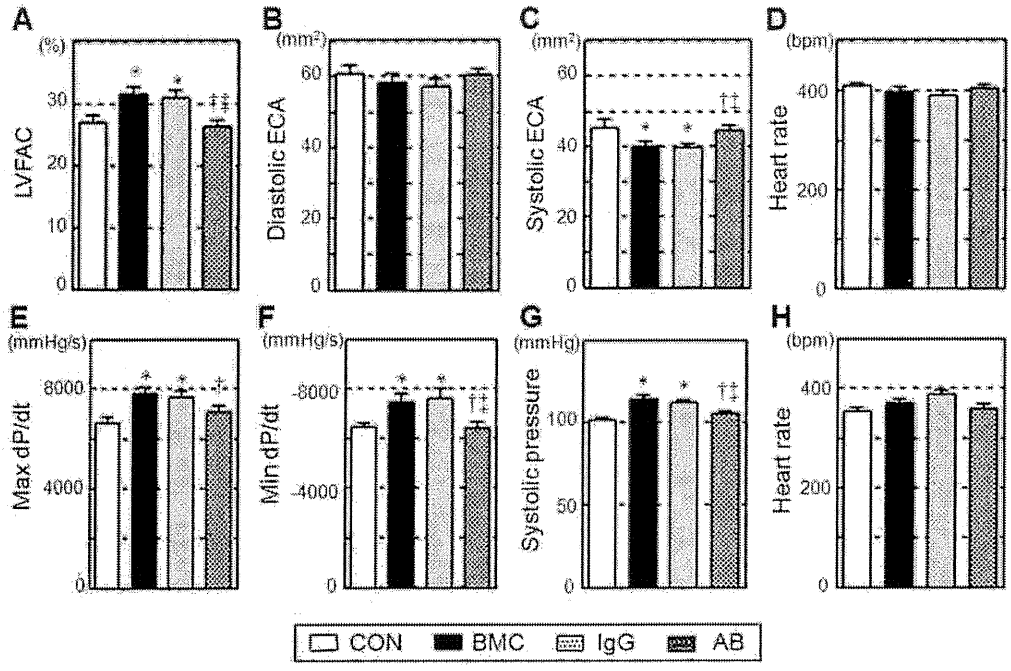

Figure 2. Abolished BMC transplantation-induced cardiac function recovery by HMGB1-inhibition. Cardiac parameters were measured by echocardiography (**A–D**) and catheterization (**E–H**) on day 28 after each treatment. Cardiac function was improved by BMC transplantation (BMC group) compared to the PBS injection control (CON group), while this effect was eliminated by antibody neutralization of HMGB1 (AB group), but not by control IgG administration (IgG group). LVFAC, left ventricular fractional area change; ECA, endocardial area. *:$p<0.05$ *versus* the CON group, †:$p<0.05$ *versus* the BMC group. ‡:$p<0.05$ *versus* the IgG group, mean±SEM for n = 8~10 in each group.
doi:10.1371/journal.pone.0076908.g002

Discussion

Using a post-MI ischemic cardiomyopathy model in rat, we demonstrated that the BMC transplantation-mediated benefits, including increased neovascular formation, reduced collagen deposition, increased proliferation activity, favorable modulation of macrophage polarization, and resultant improvement of cardiac function, were all eliminated by antibody-neutralization of HMGB1. These data suggest that extracellular HMGB1 plays a role in the effects of BMC transplantation to recover the failing myocardium undergoing post-MI adverse remodeling and to improve global cardiac function. This finding is validated by the consistency with the previous report demonstrating that administration of recombinant HMGB1 protein achieved the same benefits as the BMC transplantation-mediated effects using the similar ischemic heart failure model in rats [17].

In view of the origin of extracellular HMGB1 occurring after BMC transplantation into post MI chronic heart failure, there are 4 theoretically possible sources: (i) passive release from dead donor BMCs, (ii) passive release from dead host (endogenous) cells, (iii) active secretion from surviving donor BMCs, and (iv) active secretion from host (endogenous) cells. It is likely that the major origin may be (i) passive release from dead donor BMCs, given the following information. [I] Survival of donor BMCs was largely limited, indicating that there was a considerable amount of donor cell death; [II] In this model of ischemic cardiomyopathy, death/damage of host cells in the heart and other organs by BMC injection is unlikely to be substantial; [III] There was an increased level of circulating HMGB1 as early as 1 hour after BMC injection. This time course is too rapid for inflammatory cells to actively secrete HMGB1 *via* transcription after stimulation [9,27]. Having said these, we could not eliminate the possibility that extracellular HMGB1 from other sources, particularly from endogenous sources (host cells), might contribute to the paracrine effect of BMC transplantation. Experiments using HMGB1-deficient BMCs, either by knockout or knockdown, as donor would provide useful information to this point. However, HMGB1 knockout mice die immediately after birth [28], while on the other hand reproducible and satisfactory knockdown in primary rat unfractionated BMCs has not been established.

The role of extracellular HMGB1 to attenuate myocardial damage and to induce recovery and/or regeneration remains controversial [13–20]. This discrepancy may be relevant to different types of HMGB1 and different conditions of the host myocardium. In the settings of acute MI (without cell transplantation), a large amount of HMGB1 is actively secreted from accumulated inflammatory cells in addition to HMGB1 passively released from a large number of dead host cardiac cells. The dynamics and functions of these different types of HMGB1 are likely to be distinct, due to different phosphorylation, acetylation, and formation of complexes by binding other pathogenic molecules [9,11]. Delicate balance between these types of extracellular HMGB1 may affect the overall effect, whether beneficial or harmful, of HMGB1. Our study therefore used a post-MI ischemic cardiomyopathy model to exclude these contaminating factors. The degree of HMGB1 both from inflammatory cells and dead host cardiac cells in this model is presumed to be much less than that in acute MI settings, and the frequency of host cardiac cell death by BMC injection is also negligible, compared to donor cell death.

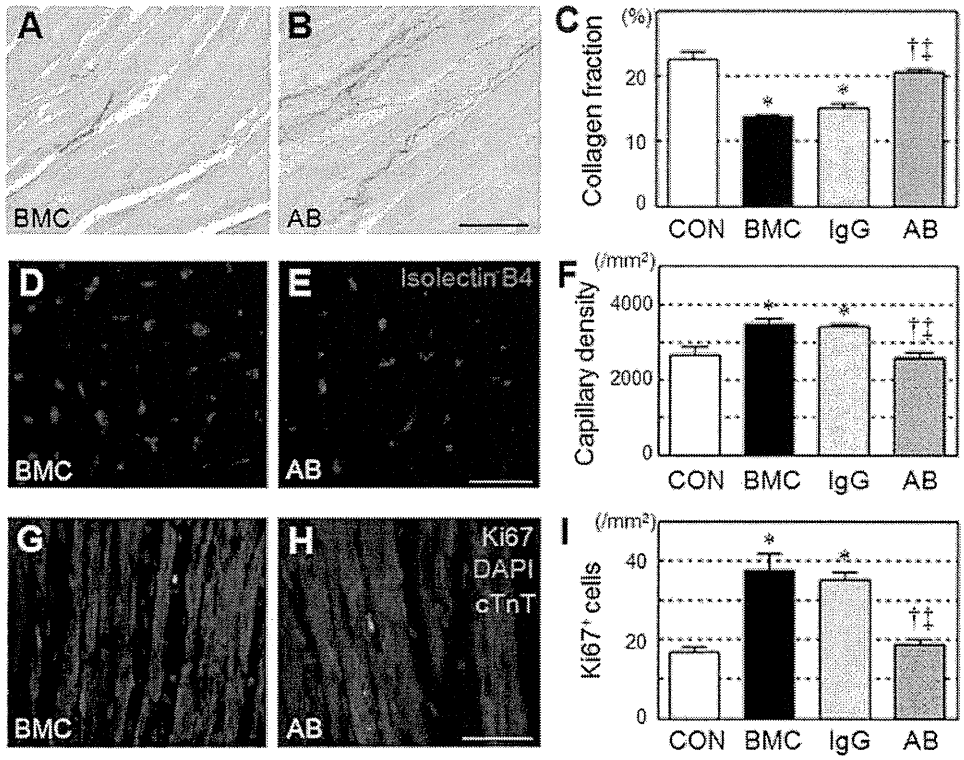

Figure 3. Eliminated BMC transplantation-induced tissue recovery by HMGB1-inhibition. Reduced extracellular collagen deposition (**A–C;** picrosirius red = red), increased capillary density (**D–F;** Isolectin B4 = red), and increased proliferation (**G–I;** Ki67 = red; nuclei = blue; cTnT = green) were observed in the border areas at day 28 after BMC transplantation (BMC group), compared to the PBS control (CON group). These effects were all abolished by anti-HMGB1 antibody neutralization (AB group), but not by control IgG administration (IgG group). Representative images of only BMC and AB groups are present (see **Figure S2** for additional images). Scale bars = 50 μm in **A, B, G, H** and 30 μm in **D, E**. *:$p<0.05$ *versus* the CON group, †:$p<0.05$ *versus* the BMC group, ‡:$p<0.05$ *versus* the IgG group, mean±SEM for n = 5~7 in each group.
doi:10.1371/journal.pone.0076908.g003

It will be interesting to investigate whether the present results in unfractionated BMCs are applicable to other types of donor cells. There are published data in other cell types that appear to be contradicting to our findings in BMCs at a glance. Ziebart *et al.* have reported that the persistence of donor cells contributes to the therapeutic effect of transplantation of endothelial progenitor cells

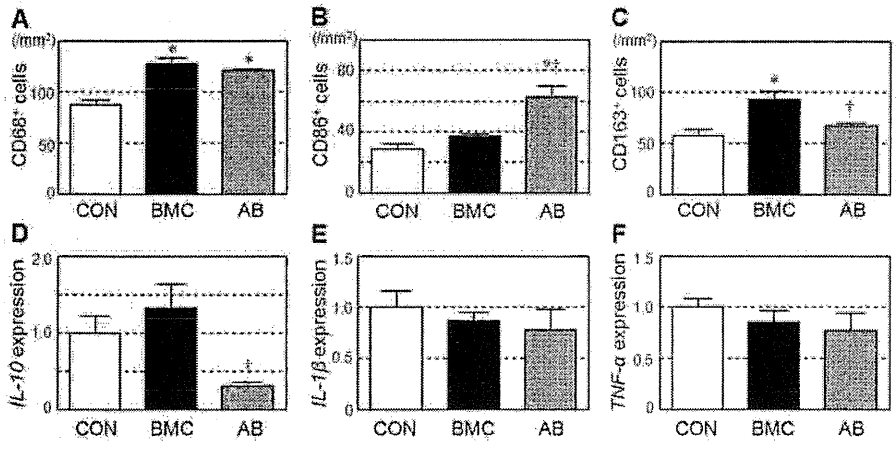

Figure 4. Modulation of innate immunity by BMC transplantation via released HMGB1. Accumulation of $CD68^+$ pan-macrophages (**A**), $CD86^+$ classically-activated pro-inflammatory M1 macrophages (**B**), and $CD163^+$ alternatively-activated anti-inflammatory M2 macrophages (**C**) in the border areas at day 3 after each treatment was assessed by immunolabeling. See **Figure S3** for representative images. Myocardial expression of *IL-10* (**D**), *IL-1β* (**E**)), and *TNF-α* (**F**) at day 3 after each treatment was measured by quantitative RT-PCR. *:$p<0.05$ *versus* the CON group, †:$p<0.05$ *versus* the BMC group, mean±SEM for n = 5~7 in each group.
doi:10.1371/journal.pone.0076908.g004

by using the inducible suicide gene [29]. Laflamme *et al.* have demonstrated that increase of donor cell presence (thus reducing donor cell death) by the treatment with pro-survival factors enhances therapeutic effects of transplantation of embryonic stem cell-derived cardiomyocytes [30]. However, in contrast, in the case of unfractionated BMCs, Yeghiazarians *et al.* reported that ultrasound-guided injection of extract of dead BMCs by freeze-thaw cycles achieves the similar therapeutic effect to injection of living BMCs [7], supporting our findings. This cell type-dependent controversy may suggest that the impact of HMGB1 released from dead donor cells to recover the damaged myocardium could be diluted/hidden in the case of transplantation of "more proficient" cells such as endothelial progenitor cells and embryonic stem cell-derived cardiomyocytes that have more substantial abilities of beneficial differentiation, secretion, and/or contraction. In addition, the extent and/or types of donor cell death after transplantation may vary according to donor cell types, affecting the release of HMGB1. Differences in the condition of the host heart, *i.e.* acute MI *versus* post-MI ischemic cardiomyopathy, may also influence the impact of extracellular HMGB1 from donor cells. Further studies to elucidate the role of extracellular HMGB1 in different donor cell types in the same experimental setting are warranted.

Macrophages are an important player in the progress and recovery of post-MI adverse ventricular remodeling [31,32]. It has also been shown that HMGB1 and receptor for advanced glycation endproducts signaling play a role in the macrophage-involved tissue repair mechanism in the peripheral nerve [33]. Recent research has shown that macrophages can be functionally polarized into classically-activated M1 (pro-inflammatory) or alternatively-activated M2 (anti-inflammation and tissue healing) phenotypes according to the environmental condition [9,26]. Stimulation with IFN-γ or TNF-α drives the macrophages into the M1 phenotype, which is characterized by a strong pro-inflammatory ability. In contrast, exposure to IL-4 or IL-13 generates M2 macrophages, which attenuate inflammation and enhance tissue recovery and healing. Importance of this polarization balance in the repair of damaged organs, including the heart, has been reported [9,26]. Our results here uncovered that BMC transplantation enhanced "beneficial" M2 macrophages in the heart, for which extracellular HMGB1 was responsible. Therefore, HMGB1-mediated modulation of the macrophage's polarization towards the M2 phenotype might be a part of the mechanism by which BMC transplantation recovers the damaged myocardium and improves cardiac function. Further study should focus on elucidation of the molecular mechanism of extracellular HMGB1 to modulate the M1/M2 macrophage polarization, in a simpler model.

A limitation of this study may be that our conclusion is based on the antibody neutralization experiments, which might carry a risk (though unlikely) of unexpected artifacts, such as unpredictable actions of the immune complexes generated. Investigations using HMGB1-deficient cells, either by knockout or knockdown, could add useful validation of our results, but these were not practical due to technical limitations as discussed above. Nonetheless, the consistency with the previous evidence that administration of HMGB1 protein induces the same effects as the BMC transplantation [17] supports our results.

In summary, our results demonstrated that extracellular HMGB1, which is derived from dead donor cells at least in part, plays a role of the effect of BMC transplantation to recover the damaged tissue by favorably modulating innate immunity in heart failure. This novel proof-of-concept will imply an important clue to further understand and refine BMC transplantation therapy for heart failure.

Supporting Information

Figure S1 Characterisation of BMCs by flow cytometry analysis. Flow cytometry analysis showed that 4.6±1.7%of collected rat BMCs were positive for CD34 and 75.5±4.3% were positive for CD45. A representative image is presented.
(TIF)

Figure S2 Supplement to Figure 3; HMGB1-inhibition abolished myocardial recovery by BMC transplantation. **A–D:** Representative images of picrosirius red staining. Scale bar = 50 μm. **E–H:** Representative images of islectin-B4 staining (red). Scale bar = 30 μm. **I–L:** Representative images of immunofluorescent labelling with Ki-67 (red); blue = nuclei (DAPI). Scale bar = 50 μm.
(TIF)

Figure S3 Supplement to Figure 4; Inflammation was modulated by BMC transplantation through HMGB1. Representative images of immunofluorescent labelling with CD68 (**A–C**), CD86 (**D–F**), and CD163 (**G–I**). Green is for each target molecule; blue for nuclei (DAPI). Scale bars = 50 μm.
(TIF)

Acknowledgments

We thank Drs Niall Campbell and Kenta Yashiro (Ken Suzuki laboratory) for their technical assistance and scientific suggestions.

Author Contributions

Conceived and designed the experiments: KS MK SRC. Performed the experiments: MK YS TN NT CI KY SF. Analyzed the data: KS MK SRC. Wrote the paper: KS MK SRC.

References

1. van Ramshorst J, Rodrigo SF, Schalij MJ, Beeres SL, Bax JJ, et al. (2011) Bone marrow cell injection for chronic myocardial ischemia: the past and the future. J Cardiovasc Transl Res 4: 182–191. doi: 10.1007/s12265-010-9249-8.
2. Donndorf P, Kundt G, Kaminski A, Yerebakan C, Liebold A, et al. (2011) Intramyocardial bone marrow stem cell transplantation during coronary artery bypass surgery: a meta-analysis. J Thorac Cardiovasc Surg 142: 911–920. doi: 10.1016/j.jtcvs.2010.12.013.
3. Fukushima S, Varela-Carver A, Coppen SR, Yamahara K, Felkin LE, et al. (2007) Direct intramyocardial but not intracoronary injection of bone marrow cells induces ventricular arrhythmias in a rat chronic ischemic heart failure model. Circulation 115: 2254–2261. doi: 10.1161/CIRCULATIONAHA.106.662577.
4. George JC, Goldberg J, Joseph M, Abdulhameed N, Crist J, et al. (2008) Transvenous intramyocardial cellular delivery increases retention in comparison to intracoronary delivery in a porcine model of acute myocardial infarction. J Interv Cardiol 21: 424–431. doi: 10.1111/j.1540-8183.2008.00390.x.
5. Ohnishi S, Yasuda T, Kitamura S, Nagaya N (2007) Effect of hypoxia on gene expression of bone marrow-derived mesenchymal stem cells and mononuclear cells. Stem Cells 25: 1166–1177. doi: 10.1634/stemcells.2006-0347.
6. Sekiguchi H, Ii M, Losordo DW (2009) The relative potency and safety of endothelial progenitor cells and unselected mononuclear cells for recovery from myocardial infarction and ischemia. J Cell Physiol 219: 235–242. doi: 10.1002/jcp.21672.
7. Yeghiazarians Y, Zhang Y, Prasad M, Shih H, Saini SA, et al. (2009) Injection of bone marrow cell extract into infarcted hearts results in functional improvement comparable to intact cell therapy. Mol Ther 17: 1250–1256. doi: 10.1038/mt.2009.85.
8. Stros M (2010) HMGB proteins: interactions with DNA and chromatin. Biochim Biophys Acta 1799: 101–113. doi: 10.1016/j.bbagrm.2009.09.008.

9. Andersson U, Tracey KJ (2011) HMGB1 is a therapeutic target for sterile inflammation and infection. Annu Rev Immunol 29: 139–162. doi: 10.1146/annurev-immunol-030409-101323.
10. Scaffidi P, Misteli T, Bianchi ME (2002) Release of chromatin protein HMGB1 by necrotic cells triggers inflammation. Nature 418: 191–195. doi: 10.1038/nature00858.
11. Yanai H, Ban T, Taniguchi T (2012) High-mobility group box family of proteins: ligand and sensor for innate immunity. Trends Immunol 33: 633–640. doi: 10.1016/j.it.2012.10.005.
12. Popovic PJ, DeMarco R, Lotze MT, Winikoff SE, Bartlett DL, et al. (2006) High mobility group B1 protein suppresses the human plasmacytoid dendritic cell response to TLR9 agonists. J Immunol 177: 8701–8707.
13. Kitahara T, Takeishi Y, Harada M, Niizeki T, Suzuki S, et al. (2008) High-mobility group box 1 restores cardiac function after myocardial infarction in transgenic mice. Cardiovasc Res 80: 40–46. doi: 10.1093/cvr/cvn163.
14. Limana F, Esposito G, D'Arcangelo D, Di Carlo A, Romani S, et al. (2011) HMGB1 attenuates cardiac remodelling in the failing heart via enhanced cardiac regeneration and miR-206-mediated inhibition of TIMP-3. PLoS One 6: e19845. doi: 10.1371/journal.pone.0019845.
15. Limana F, Germani A, Zacheo A, Kajstura J, Di Carlo A, et al. (2005) Exogenous high-mobility group box 1 protein induces myocardial regeneration after infarction via enhanced cardiac C-kit+ cell proliferation and differentiation. Circ Res 97: e73–83. doi: 10.1161/01.RES.0000186276.06104.
16. Oozawa S, Mori S, Kanke T, Takahashi H, Liu K, et al. (2008) Effects of HMGB1 on ischemia-reperfusion injury in the rat heart. Circ J 72: 1178–1184. doi: 10.1253/circj.72.1178.
17. Takahashi K, Fukushima S, Yamahara K, Yashiro K, Shintani Y, et al. (2008) Modulated inflammation by injection of high-mobility group box 1 recovers post-infarction chronically failing heart. Circulation 118: S106–114. doi: 10.1161/CIRCULATIONAHA.107.757443.
18. Zhou X, Hu X, Xie J, Xu C, Xu W, et al. (2012) Exogenous high-mobility group box 1 protein injection improves cardiac function after myocardial infarction: involvement of Wnt signaling activation. J Biomed Biotechnol 2012: 743879. doi: 10.1155/2012/743879.
19. Andrassy M, Volz HC, Igwe JC, Funke B, Eichberger SN, et al. (2008) High-mobility group box-1 in ischemia-reperfusion injury of the heart. Circulation 117: 3216–3226. doi: 10.1161/CIRCULATIONAHA.108.769331.
20. Xu H, Yao Y, Su Z, Yang Y, Kao R, et al. (2011) Endogenous HMGB1 contributes to ischemia-reperfusion-induced myocardial apoptosis by potentiating the effect of TNF-α/JNK. Am J Physiol Heart Circ Physiol 300: H913–921. doi: 10.1152/ajpheart.00703.2010.
21. Chavakis E, Hain A, Vinci M, Carmona G, Bianchi ME, et al. (2007) High-mobility group box 1 activates integrin-dependent homing of endothelial progenitor cells. Circ Res 100: 204–212. doi: 10.1161/01.RES.0000257774.55970.f4.
22. Narita T, Shintani Y, Ikebe C, Kaneko M, Harada N, et al. (2013) The use of cell-sheet technique eliminates arrhythmogenicity of skeletal myoblast-based therapy to the heart with enhanced therapeutic effects. Int J Cardiol 168: 261–269. doi: 10.1016/j.ijcard.2012.09.081.
23. Omura T, Yoshiyama M, Takeuchi K, Hanatani A, Kim S, et al. (2000) Differences in time course of myocardial mRNA expression in non-infarcted myocardium after myocardial infarction. Basic Res Cardiol 95: 316–323. doi: 10.1007/s003950070051.
24. Francic J, Weiss RM, Wei SG, Johnson AK, Felder RB (2001) Progression of heart failure after myocardial infarction in the rat. Am J Physiol Regul Integr Comp Physiol 281: R1734–1745.
25. Ouyang W, Rutz S, Crellin NK, Valdez PA, Hymowitz SG (2011) Regulation and functions of the IL-10 family of cytokines in inflammation and disease. Annu Rev Immunol 29: 71–109. doi: 10.1146/annurev-immunol-031210-101312.
26. Sica A, Mantovani A (2012) Macrophage plasticity and polarization: in vivo veritas. J Clin Invest 122: 787–795. doi: 10.1172/JCI59643.
27. Tang D, Shi Y, Jang L, Wang K, Xiao W, et al. (2005) Heat shock response inhibits release of high mobility group box 1 protein induced by endotoxin in murine macrophages. Shock 23: 434–440.
28. Calogero S, Grassi F, Aguzzi A, Voigtlander T, Ferrier P, et al. (1999) The lack of chromosomal protein Hmg1 does not disrupt cell growth but causes lethal hypoglycaemia in newborn mice. Nat Genet 22: 276–280. doi: 10.1038/10338.
29. Ziebart T, Yoon CH, Trepels T, Wietelmann A, Braun T, et al. (2008) Sustained persistence of transplanted proangiogenic cells contributes to neovascularization and cardiac function after ischemia. Circ Res 103: 1327–1334. doi: 10.1161/CIRCRESAHA.108.180463.
30. Laflamme MA, Chen KY, Naumova AV, Muskheli V, Fugate JA, et al. (2007) Cardiomyocytes derived from human embryonic stem cells in pro-survival factors enhance function of infarcted rat hearts. Nat Biotechnol 25: 1015–1024. doi: 10.1038/nbt1327.
31. Frangogiannis NG (2012) Regulation of the inflammatory response in cardiac repair. Circ Res 110: 159–173. doi: 10.1161/CIRCRESAHA.111.243162.
32. Hu Y, Zhang H, Lu Y, Bai H, Xu Y, et al. (2011) Class A scavenger receptor attenuates myocardial infarction-induced cardiomyocyte necrosis through suppressing M1 macrophage subset polarization. Basic Res Cardiol 106: 1311–1328. doi: 10.1007/s00395-011-0204-x.
33. Rong LL, Yan SF, Wendt T, Hans D, Pachydaki S, et al. (2004) RAGE modulates peripheral nerve regeneration via recruitment of both inflammatory and axonal outgrowth pathways. FASEB J 18: 1818–1825. doi: 10.1096/fj.04-1900com.

Neuroscience Research 76 (2013) 163–168

Contents lists available at SciVerse ScienceDirect

Neuroscience Research

journal homepage: www.elsevier.com/locate/neures

A highly reproducible model of cerebral ischemia/reperfusion with extended survival in CB-17 mice

Yukiko Kasahara[a], Masafumi Ihara[a], Takayuki Nakagomi[b], Yoshihiro Momota[c], David M. Stern[d], Tomohiro Matsuyama[b], Akihiko Taguchi[a,*]

[a] Department of Regenerative Medicine Research, Institute of Biomedical Research and Innovation, Hyogo, Japan
[b] Institute for Advanced Medical Sciences, Hyogo College of Medicine, Hyogo, Japan
[c] Department of Anesthesiology, Osaka Dental University, Osaka, Japan
[d] Executive Dean's Office, University of Tennessee, TN, USA

ARTICLE INFO

Article history:
Received 16 October 2012
Received in revised form 13 March 2013
Accepted 3 April 2013
Available online 18 April 2013

Keywords:
Stroke model
Transient cerebral ischemia
Ischemia/reperfusion injury
Reproducibility

ABSTRACT

To simulate the clinical and pathologic situation in patients with stroke, as well as to evaluate future potential therapeutic approaches, it is essential to have a highly reproducible model that displays long-term survival. Though a range of rodent models has been employed in the literature, there are questions regarding reproducibility, especially in terms of ischemic zone (i.e., degree of ischemia) and long-term survival. We have developed a highly reproducible stroke model that produces a consistent ischemic zone as a result of direct transient occlusion of the middle cerebral artery (MCA) in CB-17 (CB-17/Icr-+/+Jcl) mice. The model employs a thin monofilament to twist the artery resulting in complete interruption of blood flow. Transient ischemia can be induced for up to 240 min and the survival rate at 7 days post-ischemia was more than 60%, even in mice subjected to 240 min of transient ischemia resulting in hemorrhagic infarction in most animals. Our method can be used to model several pathologic conditions, such as reversible reperfusion injury, delayed neuronal death, necrotic brain injury and hemorrhagic infarction. We believe this preclinical model provides a step forward for testing future therapeutic approaches applicable to patients with ischemic brain injury.

1. Introduction

Cerebral reperfusion is known to be associated with serious brain injury, including enhanced oxidant stress/injury, hemorrhagic transformation and fatal edema. Various mechanisms, such as increased production of free radicals (Chan, 1996), disruption of the blood–brain barrier (BBB) (del Zoppo and Mabuchi, 2003), overload of critical cells with calcium ions, leukocyte accumulation in ischemic vasculature (del Zoppo et al., 1991), and subsequent infiltration of the brain parenchyma (Zhang et al., 1994), are involved in reperfusion injury. The impact of each process on cerebral injury often varies with the length and degree of ischemia. In order to simulate ischemia/reperfusion associated in clinical stroke, a highly reproducible model with long-term survival is required.

Many rodent stroke models employ an intraluminal suture for experimental ischemia/reperfusion. The latter model has the advantage of not requiring a craniotomy. However, insertion of a suture into the carotid artery interrupts blood flow to a wide territory including that of the ipsilateral MCA area, and also reduces blood flow to the ipsilateral posterior cerebral artery (PCA) and anterior cerebral artery (ACA) area, where the contralateral artery provides perfusion at a range of levels via the circle of Willis. These issues probably underlie the diminished reproducibility of the ischemic area and long-time survival in this model (Kitagawa et al., 1998; Kanemitsu et al., 2002).

Recently, we have found that the cerebral vasculature of CB-17 mice is identical comparing many animals. We have previously demonstrated that direct electrocoagulation of the M1 distal portion of the MCA in CB-17 mice induces highly reproducible and selective cortical infarction with high survival rates for extended periods (Taguchi et al., 2010). Transient ischemia can be induced by a modification of this permanent ischemia protocol (Kasahara et al., 2012). In the current manuscript, we provide detailed methods for such a new model of transient ischemia in CB-17 mice, allowing for easy replication of our work, and discuss the advantages and limitations of our model.

2. Materials and methods

All procedures were performed under auspices of an approved protocol from the Institute of Biomedical Research and Innovation Animal Care and Use Committee.

* Corresponding author at: Department of Regenerative Medicine Research, Institute of Biomedical Research and Innovation, 2-2 Minatojima-Minamimachi, Chuo-ku, Kobe 650-0047, Japan. Tel.: +81 78 304 5772; fax: +81 78 304 5263.
E-mail address: taguchi@fbri.org (A. Taguchi).

0168-0102/$ – see front matter © 2013 Elsevier Ireland Ltd and the Japan Neuroscience Society. All rights reserved.
http://dx.doi.org/10.1016/j.neures.2013.04.001

2.1. Induction of transient focal cerebral ischemia with craniotomy

Male CB-17 (CB-17/Icr-+/+Jcl) mice were purchased from Clea Japan (Tokyo, Japan). Mice were used at 7 weeks of age at weights of 22–26 g. Animals were allowed access to food and tap water ad libitum. Powdered chow and sterilized water were also provided during the first 7 days after induction of stroke.

Transient MCA occlusion was induced according to our modification of the Tamura method as described (Taguchi et al., 2010; Tamura et al., 1981). In brief, general anesthesia was induced and maintained by inhalation of 3% and 1.5% halothane (7025 Rodent Ventilator, Ugo Basile, Italy), respectively. Mice were placed in a lateral position, and a skin incision was made at the midpoint between the left orbit and the external auditory canal (Fig. 1A). Under an operating microscope (KOM300S, Konan Medical, Nishinomiya, Japan), the upper part of the temporalis muscle was pushed aside after partial resection of the left zygoma to allow visualization of the MCA through the cranial bone. A 1- to 2-mm burr hole was made using a dental drill (C710, Senko Medical Instrument Manufacturing, Tokyo, Japan), and the dura matter was opened and retracted cautiously so as not to damage the surface of the brain. Then, the MCA was isolated (Fig. 1B, lower magnification; C, higher magnification) and transiently occluded with a monofilament nylon suture distal to crossing the olfactory tract (distal M1 portion, Fig. 1D). A 2-mm length of 7–0 monofilament nylon suture (Tyco, USA), with the tip bent into a hook, was passed under the distal portion of the MCA. Subsequently, both ends of the suture were picked up and rotated 180 degrees clockwise horizontally with artery (Fig. 1E). It is notable that 7–0 nylon suture is stiffer than the artery, thus, rotation of the suture with the artery does not twist the suture but loops the artery around the suture resulting in complete interruption of blood flow (Fig. 1F). Mice were returned to cages in a controlled environment at 35–37 °C, where they were kept until reperfusion without anesthesia. After occlusion for 15, 20, 25, 120, 180, 240, 300 or 360 min, mice were placed again under anesthesia, and MCA blood flow was restored by putting the nylon suture back in place by counterclockwise rotation (Fig. 1G). During surgery, rectal temperature was monitored and controlled at 37.0 ± 0.2 °C by a feedback-regulated heating pad (ATB-1100, Nipponko-den, Tokyo, Japan). Cerebral blood flow (CBF) in the MCA area was monitored as described (Taguchi et al., 2004). Briefly, an acrylate column (Neuroscience Co., Ltd., Osaka, Japan) was attached to the intact skull using stereotactic coordinates (1 mm anterior and 3 mm lateral to the bregma), and CBF was monitored using a linear probe (1 mm in diameter) by one-dimensional laser Doppler flowmetry (Neuroscience Co., Ltd.).

2.2. Evaluation of stroke volume

At 24 and 48 h after induction of transient ischemia, mice brains were removed and sectioned coronally (1 mm thick) ($N = 8$ in each group). To evaluate the viability of brain tissue, coronal sections were incubated in 1% 2,3,5-triphenyltetrazolium (TTC: Sigma–Aldrich, St. Louis, MO) for 20 min at 37 °C in the dark and fixed in 4% paraformaldehyde/phosphate-buffered saline (PBS; pH 7.4). Infarct volume was measured using a microscopic digital camera system (Olympus, Tokyo, Japan). The TTC-positive area of each hemisphere was estimated using National Institutes of Health Image software (Version 1.62), and volume of the surviving/viable tissue was calculated by integrating the overall coronal-oriented area. Percent stroke volume was evaluated by [(contralateral hemisphere volume) − (infarcted hemisphere volume)]/[(contralateral hemisphere volume) × 2] × 100%, as described (Kasahara et al., 2012). In studies to evaluate long-term survival, 16 mice were used in each group.

2.3. Visualization of cerebral blood flow by laser speckle flowmetry

Cerebral blood flow (CBF) in the MCA area was visualized by laser speckle flowmetry (Omegazone laser speckle blood flow imager, Omegawave, Inc., Tokyo, Japan), as described previously ($N = 4$ in each group) (Nakano-Doi et al., 2010). In brief, the animal's skull was exposed and illuminated by a 780 nm semiconductor laser light. Twenty minutes of transient ischemia was induced and CBF of the same mice was sequentially evaluated at the following time points; before MCA occlusion (pre-MCAO), soon after MCA occlusion (MCAO), just before reperfusion (0 min), 5 and 60 min after reperfusion. To quantify cerebral blood flow, the region of interest (ROI) was positioned at 2.5 mm dorsal and 3 mm lateral from the bregma (i.e. the ischemic core region of MCA territory). The same grid was used to set the matching region on the contralateral side. The ratio of CBF was calculated by [(ipsilateral cerebral blood-flow)/(contralateral cerebral blood-flow)].

2.4. Data analysis

In all experiments, mean ± standard deviation is reported. JMP 8.02 (SAS Institute Inc., Co., NC, USA) was used for statistical analysis.

3. Result

3.1. Reproducible transient ischemia can be inducible up to 240 min

In a previous report, we have demonstrated a reproducible murine model of permanent cerebral ischemia by electrocoagulation of the distal portion of the MCA in CB-17 mice (Taguchi et al., 2010). In this study, we have modified the latter technique to develop a reproducible model of cerebral reperfusion injury.

All mice showed >70% decrease in cerebral blood flow rapidly after occlusion and all mice showed >80% restored cerebral blood flow soon after release of the occlusion (after 15, 20, 25, 120, 180 or 240 min of transient ischemia), compared with before transient ligation of the MCA as evaluated by one-dimensional laser Doppler flowmetry. However, rapid and reproducible reperfusion was not observed in mice after 300 or 360 min transient ischemia. Thus, mice subject to 300 or 360 min of transient ischemia were not further studied.

To investigate neuronal death after transient ischemia, brain sections were stained with TTC at 24 h after transient ischemia (Fig. 2A). No TTC-negative cerebral cortex was observed in mice after 15 min of ischemia. Only a small TTC-negative area was observed in mice subjected to 20 min of ischemia. In contrast, highly reproducible cerebral infarction was observed in all mice after 25, 120, 180 or 240 min of transient ischemia, similar to what we observed previously in the permanent MCA occlusion model (Taguchi et al., 2010). At 48 h after ischemia (Fig. 2B), there was still no TTC-negative area in mice subjected to 15 min of ischemia. In contrast, an highly reproducible TTC-negative area was observed after 20 min of ischemia, similar to that seen in mice after 25, 120, 180 or 240 min of transient ischemia. It is notable that the TTC-negative area of all samples was strictly restricted to the cerebral cortex of the MCA territory and did not include the striatum. Mean % stroke volume of each sample at 24 and 48 h after ischemia is shown in Fig. 2C and D, respectively. To confirm survival of neuronal tissue after 15 min of transient ischemia, brain sections in mice subjected to 15 min of ischemia were investigated at 7 days

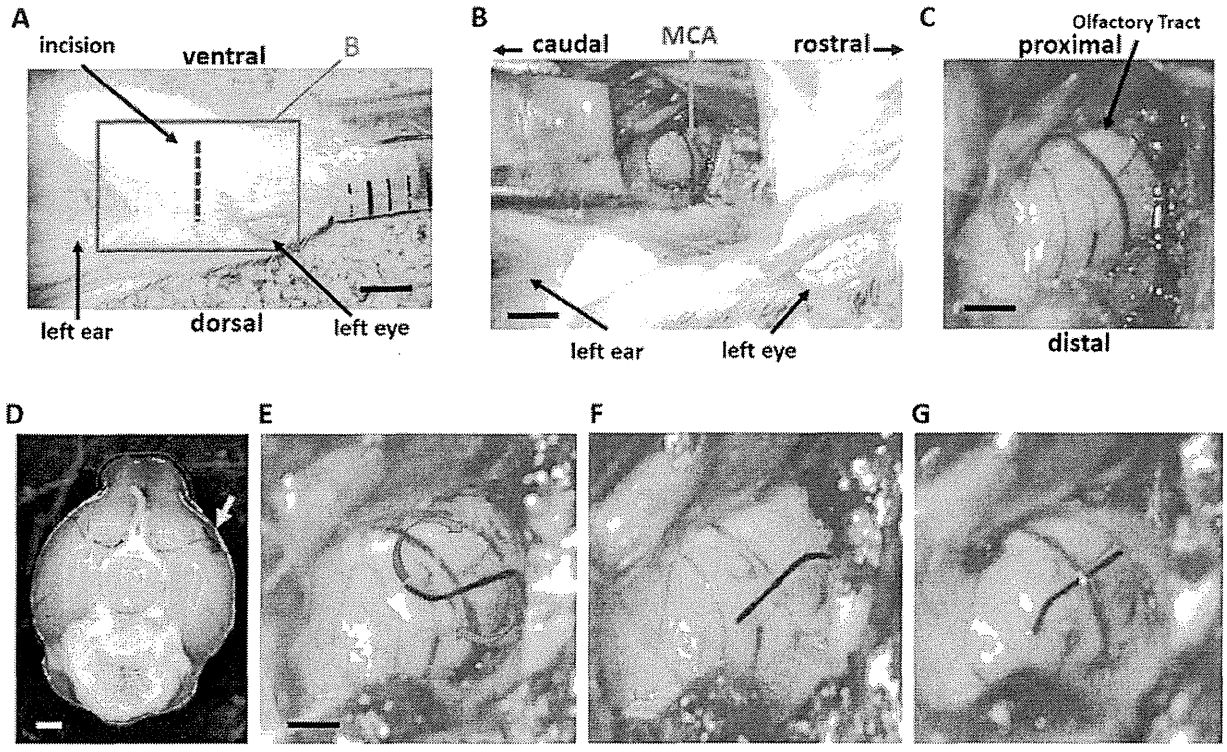

Fig. 1. Direct occlusion of the MCA followed by reperfusion. (A) Orientation of mice for induction of ischemic/reperfusion. The blue rectangle represents the enlarged area shown in panel B. (B, C) After partial resection of the left zygoma, a burr hole was made and the dura matter removed to allow isolation of the MCA (B, lower magnification; C, higher magnification). (D–F) The distal M1 portion of the MCA in CB-17 mice was directly occluded with a nylon monofilament. The arrow indicates the distal M1 portion of MCA in CB-17 mice (D). The suture was passed under the MCA and rotated 180° clockwise around the MCA (E). (F, G). Blood-flow in the distal portion of MCA was completely blocked (F). After ischemia, blood flow in the MCA was restored by putting the monofilament back into the original position (G). Scale bars, 5 mm (A), 2 mm (B), 0.6 mm (C, E) and 1.5 cm (D).

after ischemia. In the latter case, no TTC-negative area was found (not shown).

3.2. Ischemic period and hemorrhagic transformation

Hemorrhagic transformation is a life-threatening event complicating thrombolytic and/or vascular interventional therapy. Development of novel treatments to prevent hemorrhagic transformation is highly desirable for safer thrombolytic therapy that might also provide a longer therapeutic time window. Thus, using our model, at 24 h after reperfusion, the incidence and the severity of hemorrhagic infarction were investigated. Though no hemorrhagic infarction was observed in mice after ≤25 min ischemia, 90% of mice subjected to 240 min of ischemia showed hemorrhagic infarction in the MCA area (Fig. 2A and B arrow head). The incidence of hemorrhagic infarction is shown in Fig. 2E.

3.3. Ischemic period and long-term survival rate

To evaluate the therapeutic potential of novel treatments on ischemia/reperfusion injury, it is essential to investigate the outcome over longer periods (up to a week) rather than just hours after the ischemic insult. Using the intraluminal suture method, the degree of ischemia varies between areas. Thus, prolongation of the ischemic period has always been linked to variable/nonreproducible expansion of the stroke area and often results in a low survival rate during the chronic period (Memezawa et al., 1992; Popp et al., 2009). In contrast, in the current model, stroke area appears to be consistently restricted to the cerebral cortex of MCA area regardless of the period of ischemia. Fig. 3 shows survival on day 1, 3, 5 and 7 after transient ischemia. It is notable that the survival rate in mice subjected to 240 min of ischemia, where 90% of mice show hemorrhagic infarction, was more than 60% at day 7.

3.4. Temporal changes of cerebral blood flow

Two-dimensional laser speckle flowmetry analysis was employed to visualize temporal changes of cerebral blood flow (Fig. 4A–E). The decreased level of cerebral blood flow was maintained throughout the ischemic period and restored to more than 90% of the initial baseline by 5 min after the onset of reperfusion (Fig. 4F). At 60 min after reperfusion, the level of cerebral blood flow returned to that observed before MCA occlusion.

4. Discussion

In this article, we have described a highly reproducible cerebral ischemia/reperfusion model induced by direct temporal occlusion of MCA in CB-17 mice by twisting the artery using a thin monofilament. The duration of transient ischemia can be extended up to 240 min while maintaining a high survival rate at day 7 after reperfusion.

In previous studies, models of direct transient occlusion of the MCA have been described, such as those employing a micro-clip or a suture to occlude the MCA (Matsui et al., 1997; Shigeno et al., 1985). However, these models most often result in only incomplete occlusion/recirculation (Shigeno et al., 1985), and demand a very high level of surgical skill, especially in mice. Consequently, such models have gradually become less popular since the emergence of the intraluminal technique of transient MCA occlusion (Longa et al.,

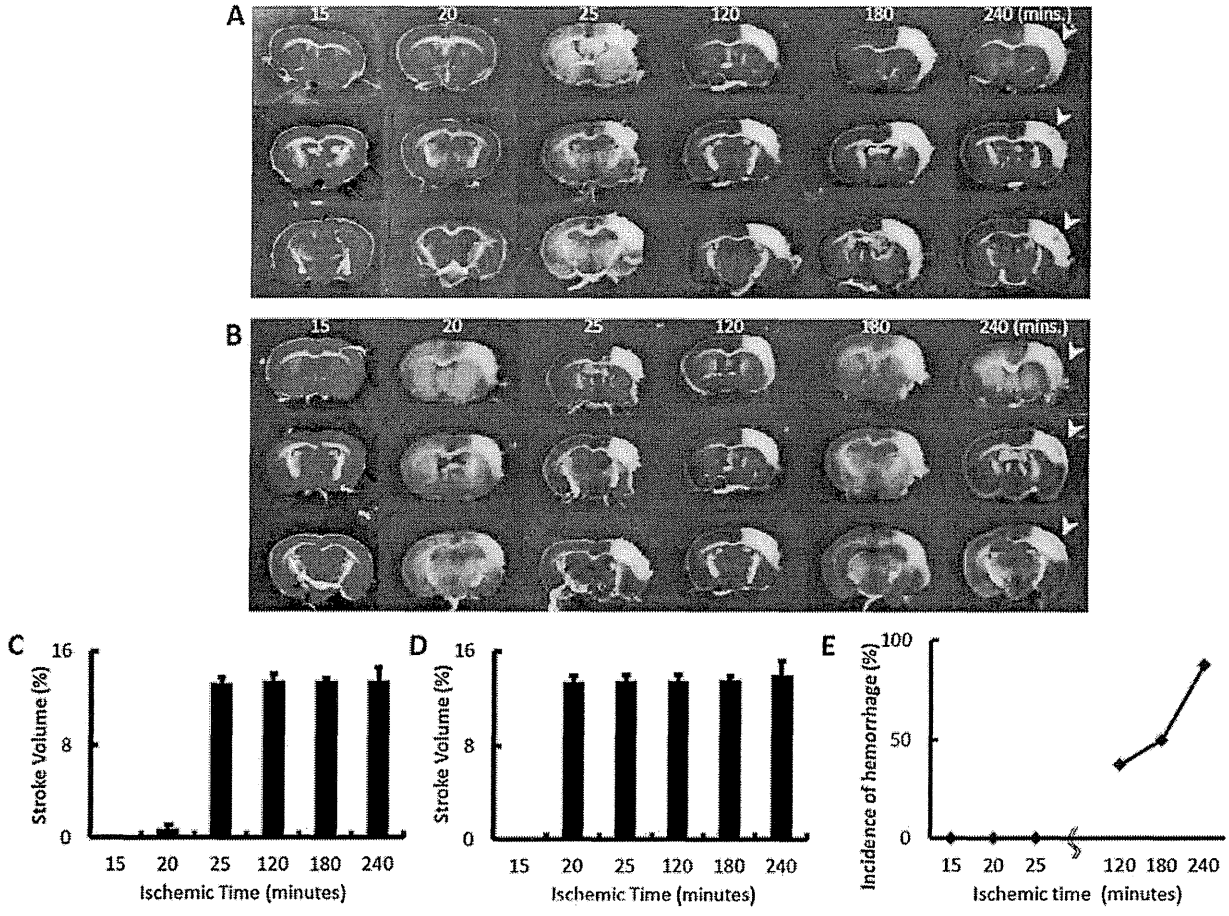

Fig. 2. Direct, transient MCA occlusion induces highly reproducible and selective cortical infarction. (A, B) Representative images of TTC-stained brain slices at 24 h (A) and 48 h (B) after ischemia/reperfusion. Though no TTC-negative area was observed after 15 min ischemia, reproducible infarction was observed after 25, 120, 180 and 240 min ischemia. It is notable that expansion of the TTC-negative area was observed at 48 h, compared with 24 h after ischemia, in mice subjected to a 20 min ischemic period. (C, D) Stroke volume at 24 h (C) and 48 h (D) after induction of ischemia. (E) Incidence of hemorrhage at 24 h after ischemia. Scale bar, 2 mm (A).

1989), the latter used as a standard for focal ischemia/reperfusion (Gomi et al., 2012; Matsuda et al., 2011; Narantuya et al., 2010). However, the intraluminal model has major disadvantages in terms of reproducibility of the area/degree of ischemia, as well as variable longer-term survival. Because the thread is inserted through left ICA, it is inevitable that blood flow is reduced to the left PCA. Furthermore, the degree flow reduction varies significantly between animals depending on the shape/placement of the thread and size of the communicating artery between the ICA and the PCA (Chiang et al., 2011; Engel et al., 2011; Kitagawa et al., 1998; Kuge et al., 1995; Longa et al., 1989; Memezawa et al., 1992). Neuronal damage may extend to the cerebral cortex and overlying the striatum depending on the time/degree of ischemia (Kanemitsu et al., 2002; Li et al., 1992; Memezawa et al., 1992). Longer periods of ischemia often cause neuronal death outside of the MCA territory, including the amygdala, hypothalamus and thalamus (Kanemitsu et al., 2002) with significant variation between animals. More extensive brain damage caused by longer ischemic periods are associated with decreased survival; the survival rate is reported to be about 10% after 240 min ischemia, respectively (Bannister and Chapman, 1984).

In contrast, direct temporal occlusion of MCA in CB-17 mice by twisting artery with thin monofilament has significant advantages.

(A) Because there is little inter-animal variation in the anatomy of the cerebral vasculature in CB-17 mice and twisting the artery with a thin monofilament completely blocks blood flow, the area and degree of ischemia are identical between animals. Such reproducibility bodes well for valid comparisons of different experimental treatments using smaller numbers of mice.

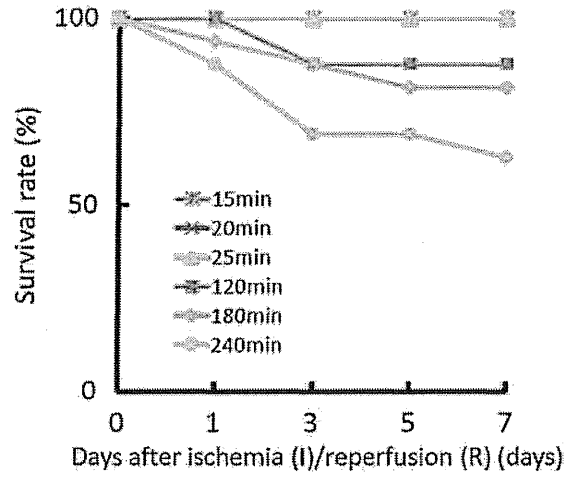

Fig. 3. Survival rate after transient ischemia. Survival rate up to 7 days after induction of transient ischemia. It is notable that the survival rate after 240 min of transient ischemia was more than 60%, even with 90% of the animals displaying hemorrhagic infarction.

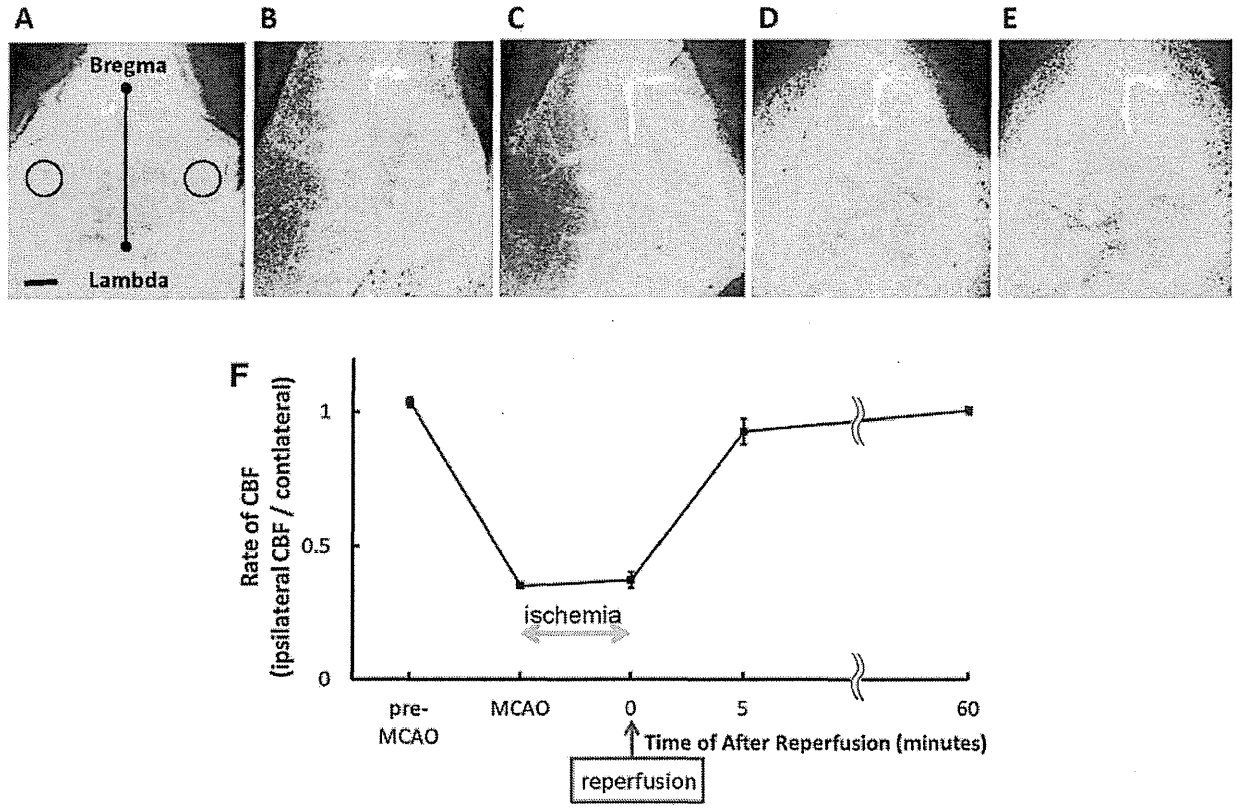

Fig. 4. Temporal changes in cerebral blood flow. (A–E) Representative pictures of two-dimensional laser speckle images before MCA occlusion (pre-MCAO: A), soon after MCA occlusion (MCAO: B), just before reperfusion (0 min: C), 5 min (D) and 60 min (E) after reperfusion. (F) The temporal changes of cerebral blood flow at ischemic core were quantified by laser speckle image. Scale bar, 1 mm (A).

(B) Because ischemic brain damage is limited to the cerebral cortex of the MCA area, survival rate at day 7 was more than 60%, even in mice subjected to 240 min of ischemia. Thus, assessment of longer-term outcomes of experimental treatments is possible.
(C) Because reproducible transient ischemia can occur for up to 240 min, a range of pathologic conditions can be modeled, including reversible reperfusion injury, delayed neuronal death, necrotic brain injury and hemorrhagic infarction.
(D) Because CB-17 mice are easy to procure, require no special diet or pre-treatment regimen and the surgical procedure is not technically demanding (compared with other methods), the current method is accessible to a wide range of investigators.

There are also short-comings of our model. The most obvious is that craniotomy results in a severe global stress to the animals, and trauma to local tissues also occurs. Sometimes, there can be small cerebral infarcts accompanying craniotomy, though these do not produce consistent functional deficits in the direct MCA occlusion model (Chen et al., 1986; Roof et al., 2001).

In conclusion, our ischemia/reperfusion model induced by twisting the MCA using a monofilament in CB-17 mice has significant advantages in reproducibility of the degree of ischemia and the ischemic area, as well as longer-term survival of the animals. Thus, it is possible to more easily test potential future therapeutic methods applicable to patients with a range of cerebral injuries using the method described herein.

Disclosures

None.

Acknowledgement

This work was supported by Japan Cardiovascular Research Foundation.

References

Bannister, C.M., Chapman, S.A., 1984. Ischemia and revascularization of the middle cerebral territory of the rat brain by manipulation of the blood vessels in the neck. Surg. Neurol. 21, 351–357.
Chan, P.H., 1996. Role of oxidants in ischemic brain damage. Stroke 27, 1124–1129.
Chen, S.T., Hsu, C.Y., Hogan, E.L., Maricq, H., Balentine, J.D., 1986. A model of focal ischemic stroke in the rat: reproducible extensive cortical infarction. Stroke 17, 738–743.
Chiang, T., Messing, R.O., Chou, W.H., 2011. Mouse model of middle cerebral artery occlusion. J. Vis. Exp. 48, 2761.
del Zoppo, G.J., Mabuchi, T., 2003. Cerebral microvessel responses to focal ischemia. J. Cereb. Blood Flow Metab. 23, 879–894.
del Zoppo, G.J., Schmid-Schonbein, G.W., Mori, E., Copeland, B.R., Chang, C.M., 1991. Polymorphonuclear leukocytes occlude capillaries following middle cerebral artery occlusion and reperfusion in baboons. Stroke 22, 1276–1283.
Engel, O., Kolodziej, S., Dirnagl, U., Prinz, V., 2011. Modeling stroke in mice – middle cerebral artery occlusion with the filament model. J. Vis. Exp. 47, 2423.
Gomi, M., Takagi, Y., Morizane, A., Doi, D., Nishimura, M., Miyamoto, S., Takahashi, J., 2012. Functional recovery of the murine brain ischemia model using human induced pluripotent stem cell-derived telencephalic progenitors. Brain Res. 1459, 52–60.
Kanemitsu, H., Nakagomi, T., Tamura, A., Tsuchiya, T., Kono, G., Sano, K., 2002. Differences in the extent of primary ischemic damage between middle cerebral artery coagulation and intraluminal occlusion models. J. Cereb. Blood Flow Metab. 22, 1196–1204.
Kasahara, Y., Nakagomi, T., Matsuyama, T., Stern, D., Taguchi, A., 2012. Cilostazol reduces the risk of hemorrhagic infarction after administration of tissue-type plasminogen activator in a murine stroke model. Stroke 43, 499–506.
Kitagawa, K., Matsumoto, M., Yang, G., Mabuchi, T., Yagita, Y., Hori, M., Yanagihara, T., 1998. Cerebral ischemia after bilateral carotid artery occlusion and intraluminal suture occlusion in mice: evaluation of the patency of the posterior communicating artery. J. Cereb. Blood Flow Metab. 18, 570–579.

Kuge, Y., Minematsu, K., Yamaguchi, T., Miyake, Y., 1995. Nylon monofilament for intraluminal middle cerebral artery occlusion in rats. Stroke 26, 1655–1657.
Li, Y., Chopp, M., Garcia, J.H., Yoshida, Y., Zhang, Z.G., Levine, S.R., 1992. Distribution of the 72-kd heat-shock protein as a function of transient focal cerebral ischemia in rats. Stroke 23, 1292–1298.
Longa, E.Z., Weinstein, P.R., Carlson, S., Cummins, R., 1989. Reversible middle cerebral artery occlusion without craniectomy in rats. Stroke 20, 84–91.
Matsuda, F., Sakakima, H., Yoshida, Y., 2011. The effects of early exercise on brain damage and recovery after focal cerebral infarction in rats. Acta Physiol. 201, 275–287.
Matsui, T., Nagafuji, T., Mori, T., Asano, T., 1997. N omega-nitro-L-arginine attenuates early ischemic neuronal damage of prolonged focal cerebral ischemia and recirculation in rats. Neurol. Res. 19, 192–203.
Memezawa, H., Smith, M.L., Siesjo, B.K., 1992. Penumbral tissues salvaged by reperfusion following middle cerebral artery occlusion in rats. Stroke 23, 552–559.
Nakano-Doi, A., Nakagomi, T., Fujikawa, M., Nakagomi, N., Kubo, S., Lu, S., Yoshikawa, H., Soma, T., Taguchi, A., Matsuyama, T., 2010. Bone marrow mononuclear cells promote proliferation of endogenous neural stem cells through vascular niches after cerebral infarction. Stem Cells 28, 1292–1302.
Narantuya, D., Nagai, A., Sheikh, A.M., Masuda, J., Kobayashi, S., Yamaguchi, S., Kim, S.U., 2010. Human microglia transplanted in rat focal ischemia brain induce neuroprotection and behavioral improvement. PLoS ONE 5, e11746.
Popp, A., Jaenisch, N., Witte, O.W., Frahm, C., 2009. Identification of ischemic regions in a rat model of stroke. PLoS ONE 4, e4764.
Roof, R.L., Schielke, G.P., Ren, X., Hall, E.D., 2001. A comparison of long-term functional outcome after 2 middle cerebral artery occlusion models in rats. Stroke 32, 2648–2657.
Shigeno, T., Teasdale, G.M., McCulloch, J., Graham, D.I., 1985. Recirculation model following MCA occlusion in rats. Cerebral blood flow, cerebrovascular permeability, and brain edema. J. Neurosurg. 63, 272–277.
Taguchi, A., Kasahara, Y., Nakagomi, T., Stern, D.M., Fukunaga, M., Ishikawa, M., Matsuyama, T., 2010. A reproducible and simple model of permanent cerebral ischemia in CB-17 and SCID mice. J. Exp. Stroke Transl. Med. 3, 28–33.
Taguchi, A., Soma, T., Tanaka, H., Kanda, T., Nishimura, H., Yoshikawa, H., Tsukamoto, Y., Iso, H., Fujimori, Y., Stern, D.M., Naritomi, H., Matsuyama, T., 2004. Administration of CD34+ cells after stroke enhances neurogenesis via angiogenesis in a mouse model. J. Clin. Invest. 114, 330–338.
Tamura, A., Graham, D.I., McCulloch, J., Teasdale, G.M., 1981. Focal cerebral ischaemia in the rat. 1. Description of technique and early neuropathological consequences following middle cerebral artery occlusion. J. Cereb. Blood Flow Metab. 1, 53–60.
Zhang, R.L., Chopp, M., Chen, H., Garcia, J.H., 1994. Temporal profile of ischemic tissue damage, neutrophil response, and vascular plugging following permanent and transient (2H) middle cerebral artery occlusion in the rat. J. Neurol. Sci. 125, 3–10.

Naritomi H, Krieger DW (eds): Clinical Recovery from CNS Damage.
Front Neurol Neurosci. Basel, Karger, 2013, vol 32, pp 69–75 (DOI: 10.1159/000346416)

Experimental Evidence and Early Translational Steps Using Bone Marrow Derived Stem Cells after Human Stroke

Yukiko Kasahara · Masafumi Ihara · Akihiko Taguchi

Department of Regenerative Medicine Research, Institute of Biomedical Research and Innovation, Kobe, Japan

Abstract

Neurogenesis is principally restricted to the subventricular zone of the lateral ventricle wall and the subgranular zone of the hippocampal dentate gyrus in physiological situations. However, neuronal stem cells are known to be mobilized into the post- and peristroke area and we have demonstrated that appropriate support of these stem cells, achieved by therapeutic angiogenesis, enhances neuroregeneration followed by neuronal functional recovery in an experimental stroke model. We also found that neural stem cells are mobilized in patients after stroke, as well as in animal models. Based on these observations, we have started cell-based therapy using autologous bone marrow-derived stem/progenitor cells in patients after stroke. This review summarizes the findings of recent experimental and clinical studies that have focused on neurogenesis in the injured brain after cerebral infarction. We also refer to the challenges for future cell-based therapy, including regeneration of the aged brain.

Stroke is the third leading cause of death in developed countries after heart disease and cancer [1], and the leading cause of disability worldwide. More than 50% of stroke survivors are unable to completely recover and 20% of stroke patients require assistance with their daily activities [2]. Although thrombolysis can improve the functional outcomes of stroke patients, patients must be treated within 3 h (or 4.5) of the onset of a stroke [3] and no definitive treatment exists after that period other than rehabilitation. To improve functional recovery after stroke, clinical trials of various drugs have been conducted but have achieved either only mild or nonsignificant therapeutic effects, or have sometimes even had serious adverse effects [4, 5]. Thus, development of novel and safe therapies is eagerly awaited.

Recently, a number of studies have focused on cell-based therapies to promote the neuronal regeneration in the ischemic brain [6–8]. In this chapter, we present current

basic and clinical findings that focus on therapeutic neurogenesis after stroke. We also refer to a novel cell-based therapy that may enable regeneration of the aged brain.

Neuronal Regeneration Is Activated after Cerebral Ischemia

Neuronal tissue in the central nervous system is well known for its limited reparative/regenerative capacity. Physiologically speaking, neurogenesis is principally restricted to the subventricular zone of the lateral ventricle wall and the subgranular zone of the hippocampal dentate gyrus, where unique niche architectures permit continuous neurogenesis [9, 10]. In pathological situations, recent studies using experimental models have revealed that endogenous neurogenesis is activated around injured areas where neurogenesis does not occur under normal conditions [11]. Consistent with these findings, histopathological studies in stroke patients have pointed out the presence of neural stem/progenitor cells in the post-stroke human cerebral cortex, and that the peak in endogenous neurogenesis occurs approximately 1–2 weeks after a stroke [12]. These findings indicate the potential for a novel therapeutic strategy using injury-induced neurogenesis for functional recovery in patients with cerebral infarction.

Angiogenesis Is Essential for the Survival of Injury-Induced Neuronal Stem Cells

The post brain-injury neurogenic response eventually yields only a very small number of mature neurons, as most of them die after the initial boosting [11]. To achieve functional recovery by endogenous neuroregeneration, appropriate support for their survival is essential and angiogenesis has been proposed as the key element in this [7]. In the adult songbird, testosterone-induced angiogenesis leads to neuronal recruitment into the higher vocal center [13]. In the adult rat, endogenous neurogenesis and neovascularization occur in proximity to one another in the cortex following focal ischemia [14]. Moreover, angiogenesis and neurogenesis have been shown to use the same molecules for their regulation; sphingosine-1-phosphate, for example, plays a critical role in neurogenesis and angiogenesis during embryonic development [15]. This accumulating evidence indicates a close relationship between the vascular system and neurogenesis in the central nervous system, and recent studies have focused on the promotion of neurogenesis in association with angiogenesis [6].

Cell-Based Therapy to Enhance Neurogenesis in Ischemic Brain

To achieve angiogenesis in ischemic tissue, an approach using bone marrow-derived mononuclear cells, a rich cell source of both hematopoietic stem cells and endothelial stem/progenitor cells, has been proposed. Local transplantation of bone marrow-

Naritomi H, Krieger DW (eds): Clinical Recovery from CNS Damage.
Front Neurol Neurosci. Basel, Karger, 2013, vol 32, pp 69–75 (DOI: 10.1159/000346416)

derived mononuclear cells in experimental models of limb ischemia significantly induces angiogenesis and releases ischemic stress in experimental models [16]. Based on these results, clinical trials were initiated, and a cure for ischemic ulcer, with significant angiogenesis in ischemic limb, has been reported [17]. The potential for transplantation of bone marrow-derived mononuclear cells to myocardial ischemia patients was also investigated and demonstrated a therapeutic effect in experimental models. Clinical trials were initiated in patients with ischemic heart disease and the therapeutic potential for improvement in regional perfusion and heart function has been reported [18].

Based on these experimental and clinical findings, we investigated the effect of intravenous transplantation of bone marrow-derived mononuclear cells [19] and hematopoietic stem cells [7] in an experimental model. As a result, we found the following three effects: (a) cell therapy enhances neovascularization at the border of the ischemic zone; (b) neovascularization is essential for the survival of injury-induced neuronal stem cells, and (c) supporting the survival of endogenous neurogenesis improves functional outcomes [19]. The positive effect of bone marrow-derived mononuclear cells was negated by administration of an anti-angiogenesis reagent [19]. It is noteworthy that survival of transplanted cells was rarely observed, despite significant activation of angiogenesis by cell therapy. These findings indicate that the differentiation of the stem cells into endothelial cells in the ischemic brain is not essential for angiogenesis after stroke and therapeutic angiogenesis could be a novel therapeutic strategy to enhance functional recovery after stroke.

To examine the effects of the mobilization of hematopoietic stem cells from bone marrow by drug administration, granulocyte colony-stimulating factor was given in an experimental stroke model and found to impair functional recovery with brain atrophy and with exaggerated inflammatory response at the border of the ischemic region [20]. This result suggested that the mobilization of bone marrow cells, including both granulocytes and hematopoietic stem cells, by granulocyte colony-stimulating factor might augment the inflammatory response consequent to ischemic tissue damage. We also investigated the effect of intravenous transplantation of bone marrow-derived mesenchymal stem cells in an experimental stroke model but found only a mild or nonsignificant effect on functional recovery (unpublished data), though mesenchymal stem cells have the potential to suppress excessive inflammation [21].

In a preclinical trial, we investigated the appropriate cell numbers and optimal therapeutic time window using a highly reproducible murine stroke model [22] and found that administration of a relatively small number of bone marrow-derived mononuclear cells had a significantly beneficial effect on the regeneration of injured brain tissue [23]. Analysis of the therapeutic time window revealed that administration of bone marrow-derived mononuclear cells at 24 h after stroke had a mild or nonsignificant effect on regeneration following ischemia, but administration of these cells between day 2 and day 14 after the ischemic event had a significantly positive effect. This result may be attributed to the time lag between the onset of stroke and the peak of neurogenesis [12].

Naritomi H, Krieger DW (eds): Clinical Recovery from CNS Damage.
Front Neurol Neurosci. Basel, Karger, 2013, vol 32, pp 69–75 (DOI: 10.1159/000346416)

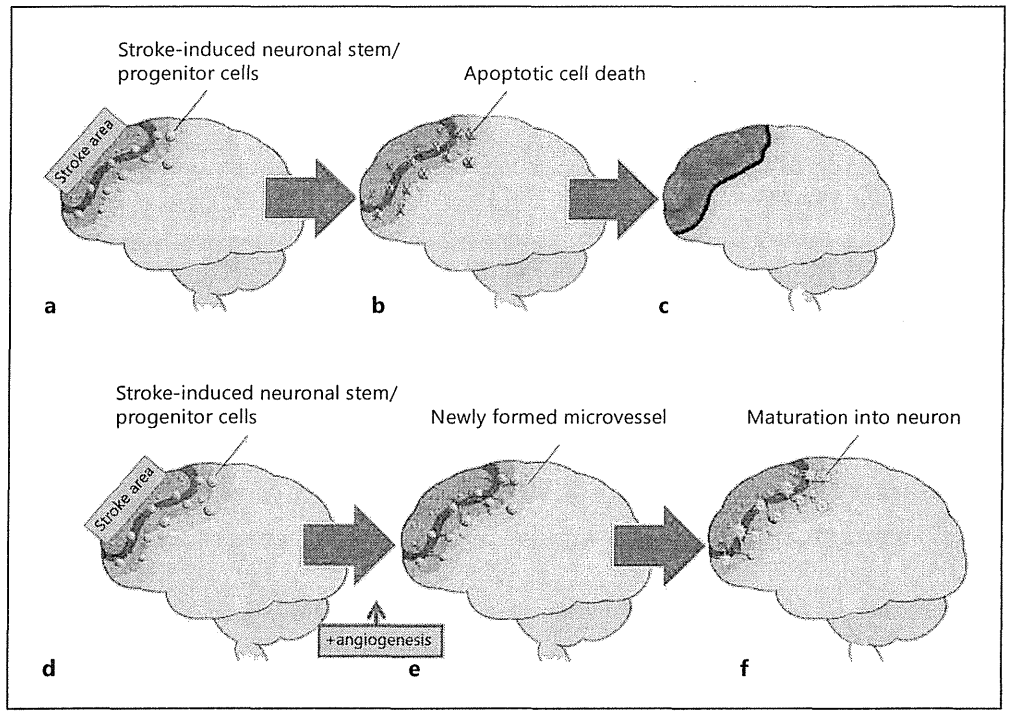

Fig. 1. Schematic representation of cell-based therapy for patients with cerebral infarction. **a–c** Neurogenesis after stroke without therapeutic angiogenesis. Endogenous neurogenesis is activated around the stroke area (**a**). However, stroke-induced neuronal stem/progenitor cells do not survive because of the lack of an appropriate environment (**b**), and do not contribute to functional recovery (**c**). **d–f** Neurogenesis with angiogenesis. Stroke-induced neuronal stem/progenitor cells (**d**) survive in an environment with angiogenesis (**e**). Neuronal stem/progenitor cells differentiate into mature neurons and contribute to functional recovery (**f**).

Clinical Trials to Enhance Neurogenesis in Patients after Stroke

Based on these results, we initiated a clinical trial to enhance neurogenesis and functional recovery through activating angiogenesis in patients with cerebral infarction. A schematic representation of this therapy is shown in figure 1. Our clinical trial is an unblinded, uncontrolled phase 1/2a study (ClinicalTrials.gov Identifier: NCT01028794). The major inclusion criteria are patients with cerebral embolism, day 7 after stroke, a National Institutes of Health Stroke Scale (NIHSS) score of more than (or equal to) 10, and an improvement in the NIHSS score of less than (or equal to) 5 since admission. On days 7–10 after stroke, either a 25-ml (low-dose group, n = 6) or a 50-ml (high-dose group, n = 6) aspiration of bone marrow cells was performed. These mononuclear cells were purified by Ficoll-Paque Premium (GE-Healthcare, USA) and administered intravenously on the day of the bone marrow aspiration. The primary outcome measures are improvement of the NIHSS score at 30 days after

Naritomi H, Krieger DW (eds): Clinical Recovery from CNS Damage.
Front Neurol Neurosci. Basel, Karger, 2013, vol 32, pp 69–75 (DOI: 10.1159/000346416)

treatment and frequency of change for the worse on the NIHSS at 30 days after treatment, compared with historical control. Though this clinical study is currently still underway, we have already treated 11 patients (6 in the low-dose and 5 in the high-dose group), and no side effects or safety problems have been observed to date. Results related to the therapeutic effects of the treatment are expected in a year. Similar clinical trials are being carried out in other countries, including the USA, UK, Brazil and Spain, with promising results [24, 25]. Though the route of administration (intravenous or intra-arterial) and cell source (bone marrow mononuclear cells or CD34-positive cells) vary, no side effects or safety problems with cell therapy have been reported. The current status of most of these ongoing clinical trials can be searched through http://clinicaltrials.gov/.

Future Cell-Based Therapy for Prevention of Cerebrovascular Diseases

Previously, we have shown that patients with cerebrovascular disease have a decreased level of circulating bone marrow-derived immature cells, the latter associated with impaired cerebrovascular function [26] and impaired cognition [27], whereas increased levels of bone marrow-derived immature cells are associated with neovascularization of the ischemic brain [28]. In addition, we have demonstrated that partial rejuvenation of bone marrow stem cells in aged rats improves vascular function and reduces ischemic damage after induction of stroke in stroke-prone spontaneously hypertensive rats [29]. Furthermore, we investigated the effect of bone marrow-derived stem cells on white matter damage in a mouse model of cerebral hypoperfusion and found that administration of bone marrow-derived stem cells has a significant protective effect against white matter damage by enhancing cerebral blood flow via the activation of nitric oxide synthase [30]. These findings clearly indicate that bone marrow-derived stem/immature cells have the potential to improve microvascular circulation and prevent cerebrovascular diseases, and the challenge to find novel strategies using autologous, allogeneic or induced pluripotent stem cell-derived hematopoietic stem cells to regenerate the aged brain is ongoing.

Conclusion

Currently, for patients after stroke, there is no specific recovery-targeted treatment other than physical and cognitive rehabilitation techniques after the period of thrombolysis. However, accumulating evidence indicates significant activation of neurogenesis after stroke, and utilization of the stroke-induced neuronal stem cells, we believe, will become a major therapeutic target for the acceleration of functional recovery. The mechanism that links angiogenesis and neurogenesis cannot be attributed to a single molecule or signaling pathway. It is likely that multiple cytokines,

Naritomi H, Krieger DW (eds): Clinical Recovery from CNS Damage.
Front Neurol Neurosci. Basel, Karger, 2013, vol 32, pp 69–75 (DOI: 10.1159/000346416)

growth factors, and cell adhesion molecules are involved, and the balance between these molecules may determine the fate of injured brain tissue. Careful, step-by-step investigation will lead to more efficient neurogenesis with a longer therapeutic time window. Experimental and clinical research focusing on neuroregeneration is needed to enhance functional recovery in patients after stroke.

References

1 Pearson TA: Cardiovascular disease in developing countries: myths, realities, and opportunities. Cardiovasc Drugs Ther 1999;13:95–104.
2 Bonita R, Solomon N, Broad JB: Prevalence of stroke and stroke-related disability. Estimates from the Auckland stroke studies. Stroke 1997;28:1898–1902.
3 Hacke W, Donnan G, Fieschi C, Kaste M, von Kummer R, Broderick JP, Brott T, Frankel M, Grotta JC, Haley EC Jr, Kwiatkowski T, Levine SR, Lewandowski C, Lu M, Lyden P, Marler JR, Patel S, Tilley BC, Albers G, Bluhmki E, Wilhelm M, Hamilton S: Association of outcome with early stroke treatment: pooled analysis of ATLANTIS, ECASS, and NINDS rt-PA stroke trials. Lancet 2004;363:768–774.
4 Adams HP Jr, Adams RJ, Brott T, del Zoppo GJ, Furlan A, Goldstein LB, Grubb RL, Higashida R, Kidwell C, Kwiatkowski TG, Marler JR, Hademenos GJ, Stroke Council of the American Stroke A: Guidelines for the early management of patients with ischemic stroke: a scientific statement from the Stroke Council of the American Stroke Association. Stroke 2003; 34:1056–1083.
5 Sandercock PA, Soane T: Corticosteroids for acute ischaemic stroke. Cochrane Database Syst Rev 2011; 9:CD000064.
6 Nakagomi N, Nakagomi T, Kubo S, Nakano-Doi A, Saino O, Takata M, Yoshikawa H, Stern DM, Matsuyama T, Taguchi A: Endothelial cells support survival, proliferation, and neuronal differentiation of transplanted adult ischemia-induced neural stem/progenitor cells after cerebral infarction. Stem Cells 2009;27:2185–2195.
7 Taguchi A, Soma T, Tanaka H, Kanda T, Nishimura H, Yoshikawa H, Tsukamoto Y, Iso H, Fujimori Y, Stern DM, Naritomi H, Matsuyama T: Administration of CD34+ cells after stroke enhances neurogenesis via angiogenesis in a mouse model. J Clin Invest 2004;114:330–338.
8 Takahashi K, Yasuhara T, Shingo T, Muraoka K, Kameda M, Takeuchi A, Yano A, Kurozumi K, Agari T, Miyoshi Y, Kinugasa K, Date I: Embryonic neural stem cells transplanted in middle cerebral artery occlusion model of rats demonstrated potent therapeutic effects, compared to adult neural stem cells. Brain Res 2008;1234:172–182.
9 Alvarez-Buylla A, Garcia-Verdugo JM: Neurogenesis in adult subventricular zone. J Neurosci 2002;22: 629–634.
10 Gage FH: Molecular and cellular mechanisms contributing to the regulation, proliferation and differentiation of neural stem cells in the adult dentate gyrus. Keio J Med 2010;59:79–83.
11 Arvidsson A, Collin T, Kirik D, Kokaia Z, Lindvall O: Neuronal replacement from endogenous precursors in the adult brain after stroke. Nat Med 2002;8:963–970.
12 Nakayama D, Matsuyama T, Ishibashi-Ueda H, Nakagomi T, Kasahara Y, Hirose H, Kikuchi-Taura A, Stern DM, Mori H, Taguchi A: Injury-induced neural stem/progenitor cells in post-stroke human cerebral cortex. Eur J Neurosci 2010;31:90–98.
13 Louissaint A Jr, Rao S, Leventhal C, Goldman SA: Coordinated interaction of neurogenesis and angiogenesis in the adult songbird brain. Neuron 2002;34: 945–960.
14 Shin HY, Kim JH, Phi JH, Park CK, Kim JE, Kim JH, Paek SH, Wang KC, Kim DG: Endogenous neurogenesis and neovascularization in the neocortex of the rat after focal cerebral ischemia. J Neurosci Res 2008;86:356–367.
15 Mizugishi K, Yamashita T, Olivera A, Miller GF, Spiegel S, Proia RL: Essential role for sphingosine kinases in neural and vascular development. Mol Cell Biol 2005;25:11113–11121.
16 Shintani S, Murohara T, Ikeda H, Ueno T, Sasaki K, Duan J, Imaizumi T: Augmentation of postnatal neovascularization with autologous bone marrow transplantation. Circulation 2001;103:897–903.
17 Kirana S, Stratmann B, Prante C, Prohaska W, Koerperich H, Lammers D, Gastens MH, Quast T, Negrean M, Stirban OA, Nandrean SG, Gotting C, Minartz P, Kleesiek K, Tschoepe D: Autologous stem cell therapy in the treatment of limb ischaemia induced chronic tissue ulcers of diabetic foot patients. Int J Clin Pract 2012;66:384–393.
18 Moreira Rde C, Haddad AF, Silva SA, Souza AL, Tuche FA, Oliveira MA, Mesquita CT, Rochitte CE, Borojevic R, Dohmann HF: Intracoronary stem-cell injection after myocardial infarction: microcirculation sub-study. Arq Bras Cardiol 2011;97:420–426.

Naritomi H, Krieger DW (eds): Clinical Recovery from CNS Damage.
Front Neurol Neurosci. Basel, Karger, 2013, vol 32, pp 69–75 (DOI: 10.1159/000346416)

19 Nakano-Doi A, Nakagomi T, Fujikawa M, Nakagomi N, Kubo S, Lu S, Yoshikawa H, Soma T, Taguchi A, Matsuyama T: Bone marrow mononuclear cells promote proliferation of endogenous neural stem cells through vascular niches after cerebral infarction. Stem Cells 2010;28:1292–1302.
20 Taguchi A, Wen Z, Myojin K, Yoshihara T, Nakagomi T, Nakayama D, Tanaka H, Soma T, Stern DM, Naritomi H, Matsuyama T: Granulocyte colony-stimulating factor has a negative effect on stroke outcome in a murine model. Eur J Neurosci 2007;26:126–133.
21 Tsuda H, Yamahara K, Ishikane S, Otani K, Nakamura A, Sawai K, Ichimaru N, Sada M, Taguchi A, Hosoda H, Tsuji M, Kawachi H, Horio M, Isaka Y, Kangawa K, Takahara S, Ikeda T: Allogenic fetal membrane-derived mesenchymal stem cells contribute to renal repair in experimental glomerulonephritis. Am J Physiol Renal Physiol 2010;299:F1004–F1013.
22 Taguchi A, Kasahara Y, Nakagomi T, Stern DM, Fukunaga M, Ishikawa M, Matsuyama T: A reproducible and simple model of permanent cerebral ischemia in CB-17 and SCID mice. J Exp Stroke Transl Med 2010;3:28–33.
23 Uemura M, Kasahara Y, Nagatsuka K, Taguchi A: Cell-based therapy to promote angiogenesis in the brain following ischemic damage. Curr Vasc Pharmacol 2012;10:285–288.
24 Savitz SI, Misra V, Kasam M, Juneja H, Cox CS Jr, Alderman S, Aisiku I, Kar S, Gee A, Grotta JC: Intravenous autologous bone marrow mononuclear cells for ischemic stroke. Ann Neurol 2011;70:59–69.
25 Battistella V, de Freitas GR, da Fonseca LM, Mercante D, Gutfilen B, Goldenberg RC, Dias JV, Kasai-Brunswick TH, Wajnberg E, Rosado-de-Castro PH, Alves-Leon SV, Mendez-Otero R, Andre C: Safety of autologous bone marrow mononuclear cell transplantation in patients with nonacute ischemic stroke. Regen Med 2011;6:45–52.
26 Taguchi A, Matsuyama T, Moriwaki H, Hayashi T, Hayashida K, Nagatsuka K, Todo K, Mori K, Stern DM, Soma T, Naritomi H: Circulating CD34-positive cells provide an index of cerebrovascular function. Circulation 2004;109:2972–2975.
27 Taguchi A, Nakagomi N, Matsuyama T, Kikuchi-Taura A, Yoshikawa H, Kasahara Y, Hirose H, Moriwaki H, Nakagomi T, Soma T, Stern DM, Naritomi H: Circulating CD34-positive cells have prognostic value for neurologic function in patients with past cerebral infarction. J Cereb Blood Flow Metab 2009;29:34–38.
28 Yoshihara T, Taguchi A, Matsuyama T, Shimizu Y, Kikuchi-Taura A, Soma T, Stern DM, Yoshikawa H, Kasahara Y, Moriwaki H, Nagatsuka K, Naritomi H: Increase in circulating CD34-positive cells in patients with angiographic evidence of moyamoya-like vessels. J Cereb Blood Flow Metab 2008;28:1086–1089.
29 Taguchi A, Zhu P, Cao F, Kikuchi-Taura A, Kasahara Y, Stern DM, Soma T, Matsuyama T, Hata R: Reduced ischemic brain injury by partial rejuvenation of bone marrow cells in aged rats. J Cereb Blood Flow Metab 2011;31:855–867.
30 Fujita Y, Ihara M, Ushiki T, Hirai H, Kizaka-Kondoh S, Hiraoka M, Ito H, Takahashi R: Early protective effect of bone marrow mononuclear cells against ischemic white matter damage through augmentation of cerebral blood flow. Stroke 2010;41:2938–2943.

Akihiko Taguchi
Department of Regenerative Medicine Research
Institute of Biomedical Research and Innovation
2–2 Minatojima-Minamimachi, Chuo-ku, Kobe 650–0047 (Japan)
E-Mail taguchi@fbri.org

Naritomi H, Krieger DW (eds): Clinical Recovery from CNS Damage.
Front Neurol Neurosci. Basel, Karger, 2013, vol 32, pp 69–75 (DOI: 10.1159/000346416)

Experimental Neurology 247 (2013) 218–225

Contents lists available at SciVerse ScienceDirect

Experimental Neurology

journal homepage: www.elsevier.com/locate/yexnr

A novel reproducible model of neonatal stroke in mice: Comparison with a hypoxia–ischemia model

Masahiro Tsuji [a,*], Makiko Ohshima [a], Akihiko Taguchi [a,b], Yukiko Kasahara [b], Tomoaki Ikeda [c], Tomohiro Matsuyama [d]

[a] Department of Regenerative Medicine and Tissue Engineering, National Cerebral and Cardiovascular Center Research Institute, 5-7-1, Fujishiro-dai, Suita, Osaka, 565-8565, Japan
[b] Department of Regenerative Medicine, Institute of Biomedical Research and Innovation, 2-2, Minami-machi, Minatojima, Chuo-ku, Kobe, 650-0047, Japan
[c] Department of Obstetrics and Gynecology, Mie University School of Medicine, 2-174, Edobashi, Tsu, Mie, 514-8507, Japan
[d] Laboratory of Neurogenesis and CNS Repair, Institute for Advanced Medical Science, Hyogo College of Medicine, 1-1, Mukogawacho, Nishinomiya, Hyogo, 663-8501, Japan

ARTICLE INFO

Article history:
Received 18 January 2013
Revised 1 April 2013
Accepted 18 April 2013
Available online 4 May 2013

Keywords:
Neonatal stroke
Neonatal encephalopathy
Focal ischemia
Middle cerebral artery occlusion
Hypoxic–ischemic encephalopathy
CB-17 mouse
Variability

ABSTRACT

Neonatal stroke occurs in 1/4000 live births and leaves life-long neurological impairments, such as cerebral palsy and epilepsy. Currently, the rodent models of neonatal stroke that are available exhibit significant inter-animal variability, which makes it difficult to accurately assess the mechanisms of brain injury and the efficacy of candidate treatments. We aimed to introduce a novel, highly reproducible model of stroke, middle cerebral artery occlusion (MCAO), in immature mice, and to evaluate the reproducibility of this model compared with a conventional hypoxia–ischemia (HI) model. Postnatal day 12 CB-17 mice underwent left MCAO by direct electrocoagulation. The MCAO model exhibited excellent long-term survival; 85% up to 8 weeks after the insult. Infarct was evident in every animal with MCAO ($n = 27$) and was confined to the cortex, with the exception of some mild thalamic injury. While the % stroke volume 48 h after the insult was consistent in the MCAO group, range: 17.8–30.4% (minimum–maximum), it was substantially less consistent in the HI group, range: 3.0–70.1%. This contrasting variability between the two models was also evident in the cerebral blood flow, 24 h after the insult, and in the ipsilateral hemispheric volume, as assessed at 8 weeks after the insult. Mice with MCAO exhibited significant neurofunctional deficits in the rotarod and open-field tests. Preclinical studies for neonatal stroke could become more reliable using this model, with even a potential reduction in the number of pups required for statistical significance. The contrasting variability between the two models may provide insights into the factors that contribute to inter-animal variability in brain injury.

Introduction

Perinatal/neonatal arterial ischemic stroke occurs in 1/2800 to 1/5000 live births, has a mortality rate of 2–10%, and leaves life-long neurological impairments, such as cerebral palsy, cognitive delay, and epilepsy (Chabrier et al., 2011; Golomb et al., 2006; Nelson and Lynch, 2004). The common early symptoms are seizures, persistently altered muscle tone, and decreased consciousness (Chabrier et al., 2011). Most perinatal arterial ischemic events occur in the region of the middle cerebral artery (MCA), with a left-hemisphere predominance (Lee et al., 2005; Sreenan et al., 2000). While full-term infants tend to exhibit occlusion of the main branch, preterm infants tend to exhibit occlusions of a cortical branch or one or more of the lenticulostriate branches (de Vries et al., 1997). There is currently no evidence-based treatment for neonates with stroke (Chabrier et al., 2011). Furthermore, the average 5-year direct medical cost for neonatal stroke is approximately $52,000 US (Gardner et al., 2010).

When investigating brain injuries, it is essential to utilize a highly reproducible model of brain injury. The model has to provide: 1) an accurate neurological evaluation, 2) a detailed evaluation of the injury/neuroprotection mechanisms, and 3) limitation in the numbers of animals used. Several neonatal stroke models have been developed using artery obstruction (Ashwal et al., 1995; Comi et al., 2004; Derugin et al., 1998; Mitsufuji et al., 1996; Renolleau et al., 1998; Wen et al., 2004). Almost all of these models exhibit significant inter-animal variability in the extent of the brain injury; i.e. a subset of pups exhibit no perceivable brain injury.

Neonatal encephalopathy (NE) is a neonatal neurological syndrome with clinical features that include decreased consciousness –

Abbreviations: MCA, middle cerebral artery; MCAO, middle cerebral artery occlusion; NE, neonatal encephalopathy; HIE, hypoxic–ischemic encephalopathy; HI, hypoxic–ischemic, hypoxia–ischemia; CBF, cerebral blood flow; ANOVA, analysis of variance.

* Corresponding author. Fax: +81 6 6835 5496.
E-mail addresses: tsuji.masahiro.ri@mail.ncvc.go.jp (M. Tsuji), oshima.makiko.ri@mail.ncvc.go.jp (M. Ohshima), taguchi@fbri.org (A. Taguchi), kasahara@fbri.org (Y. Kasahara), t-ikeda@clin.medic.mie-u.ac.jp (T. Ikeda), tomohiro@hyo-med.ac.jp (T. Matsuyama).

0014-4886/$ – see front matter © 2013 Elsevier Inc. All rights reserved.
http://dx.doi.org/10.1016/j.expneurol.2013.04.015

usually associated with respiratory depression, altered muscle tone, disturbances of cranial nerve function – especially impaired feeding, and often seizures (Volpe, 2012). The most common etiology of NE is cerebral ischemia; hypoxic–ischemic encephalopathy (HIE) 50–80%, and stroke ~5–10% (Volpe, 2012), NE encompasses HIE and stroke. Recently, some authors have proposed that the term HIE should not be used in practice and should be replaced by the more general term, NE, for a number of reasons (Dammann et al., 2011), whereas other authors have opposed this proposal (Volpe, 2012). The most widely-used HIE model is the Rice–Vannucci model, which combines permanent unilateral ligation of the carotid artery in 7-day-old rat pups, along with exposure to hypoxia (Johnston et al., 2005; Rice et al., 1981). It is important to note that this model also exhibits significant inter-animal variability in the extent of the brain injury (Aden et al., 2002; Sheldon et al., 1998).

Some neonates with stroke can present signs and symptoms similar to HIE, and vice-versa. Moreover, some babies may exhibit both etiologies, and it is often difficult to isolate the cause of NE. Therefore, it is important to understand the differences between arterial ischemic stroke and hypoxia–ischemia (HI). Nevertheless, to the best of our knowledge, only one study (Ashwal et al., 2007) has directly compared the HI model in immature animals and a stroke model in immature animals to date.

We have previously developed a highly reproducible model of adult stroke induced by direct electrocoagulation of the unilateral MCA in CB-17 (CB-17/Icr-+/+Jcl) and SCID (CB-17/Icr-scid/scidJcl) mice (Taguchi et al., 2004, 2010). Recently, we adapted the same technique to immature CB-17 mice, and have succeeded in developing a model of neonatal stroke that shows remarkable consistency of the brain injury. The objectives of our study were: 1) to introduce a novel model of stroke in immature mice and 2) to test reproducibility of this model as compared to the HI model.

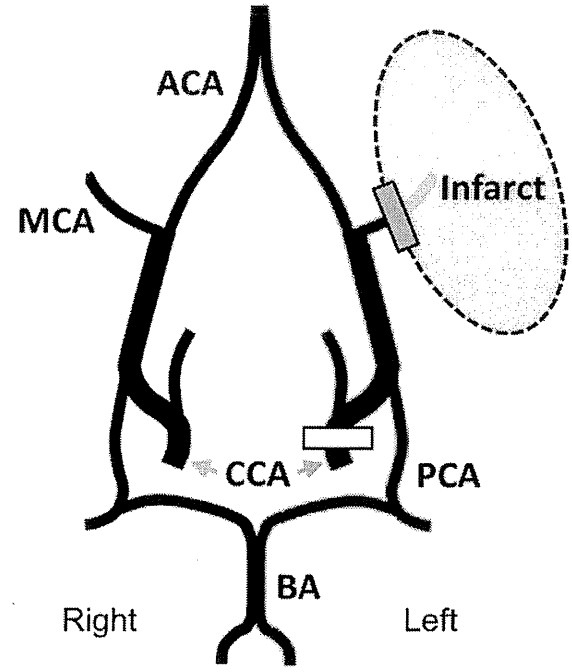

Fig. 1. Representation of the circle of Willis in rodents. The anatomic arterial system at the base of the brain in horizontal projection. ACA; anterior cerebral artery. BA; basilar artery. CCA; common carotid artery. MCA; middle cerebral artery. PCA; posterior cerebral artery. In the MCA occlusion model, the left MCA is permanently occluded (gray box). In the hypoxia–ischemia model, the left CCA is permanently occluded (open box) followed by transient systemic exposure to hypoxia.

Methods

Animals and surgeries

Postnatal day 12 (P12) male and female CB-17 mouse pups (n = 94, weight: 6.7 ± 1.2 g) (CLEA Japan Inc., Tokyo, Japan) were prepared for surgery. P8–12 mice are considered comparable to human term (P0) neonates with regard to brain maturation (Hagberg et al., 2002). All experiments were performed in accordance with protocols approved by the Experimental Animal Care and Use Committee of the National Cerebral and Cardiovascular Center.

Permanent MCA occlusion (MCAO) was produced by a modification of the adult MCAO model that we have reported previously (Taguchi et al., 2010) (Fig. 1). A skin incision was made between the left eye and ear under isoflurane anesthesia (4.0% for induction, 1.5–2.0% for maintenance). The zygoma was dissected to visualize the MCA through the cranial bone. A hole was made in the temporal bone by removing a portion of it using fine forceps. The left MCA was electrocauterized, and disconnected just distal to its crossing of the olfactory tract (distal M1 portion). The average duration of the whole procedure was approximately 15 min. HI was induced by a combination of permanent occlusion of the left common carotid artery and exposure to 8% oxygen for 30 min in the P12 CB-17 mice, as described previously (Ohshima et al., 2012) (Fig. 1). Sham-surgery controls underwent open-skull surgery without MCA electrocoagulation. To properly assess the differences in variability between the two models, a single researcher, the first author, performed all surgical procedures. All analyses were performed by investigators who were blinded to the experimental group.

Cerebral blood flow measurements

The cortical surface cerebral blood flow (CBF) was measured by a laser speckle flowmetry imaging system (Omegawave Inc., Tokyo, Japan) immediately before and 24 h after MCAO or HI, as described previously, with a minor modification (Ohshima et al., 2012). CBF was measured through the intact skull with an open-scalp.

Behavioral tests

Sensorimotor skills were evaluated 2 weeks after the insult (P26) using the rotarod test, as rodents with brain damage have been reported to exhibit behavioral impairment at this time point (Jansen and Low, 1996). The rotarod accelerated from 4 to 40 rpm over 5 min (Muromachi Kikai Co., Ltd., Tokyo, Japan). The time until the mouse fell off the rotating drum was recorded in 5 consecutive sessions, and the average time spent on the drum was used for statistical comparison.

Locomotor and exploratory behaviors were evaluated 5 weeks after the insults (almost 7 weeks of age) using the open-field test, as in our preliminary study mice began to respond to a dark environment from this age onward. Animals were allowed to search freely in a box (30 × 30 cm) for 30-min in a light environment and for the subsequent 30-min in a dark environment (Taiyo Electric Co., Ltd, Osaka, Japan). On the X-, Y-, and Z-banks of the open-field, infrared beams were mounted at specific intervals. The total number of beam crossings by the animal was counted and scored as "locomotion" for the horizontal movement, and as "rearing" for the vertical movement. Both behavioral tests were repeated one week before sacrifice at 8 weeks after the insult.